

ROSAT OBSERVATIONS OF FIVE CHROMOSPHERICALLY ACTIVE STARS

K. P. SINGH,¹ S. A. DRAKE,² AND N. E. WHITE

Code 660.2, Laboratory for High Energy Astrophysics, NASA/GSFC, Greenbelt, Maryland 20771

Electronic mail: singh@tifrvax.tifr.res.in, drake@lheavx.gsfc.nasa.gov, white@adhoc.gsfc.nasa.gov

THEODORE SIMON

Institute for Astronomy, University of Hawaii, 2680 Woodlawn Drive, Honolulu, Hawaii 96822

Electronic mail: simon@hubble.ifa.hawaii.edu

Received 1995 December 28; revised 1995 March 26

ABSTRACT

We present x-ray spectra of three chromospherically active binaries, HR 7428, FF Aqr, and IX Per, and two active giant stars, 29 Dra and HR 9024. The spectra were obtained using the Position Sensitive Proportional Counter (PSPC) on the *ROSAT* satellite. For coronal plasma models with 1-temperature or 2-temperature components, we find that a range of heavy element abundances, from solar to extreme sub-solar abundances similar to those that have been inferred from analyses of *ASCA* spectra, provide acceptable fits to the observed PSPC spectra. The highest signal-to-noise spectrum of 29 Dra requires either a 1- or 2-temperature model with greatly sub-solar (photospheric) abundances or else a 3-component model with solar abundances. The degeneracy of these results, i.e., the fact that quite different models can produce acceptable fits to the PSPC spectra, means that it is difficult to infer the temperature structure of a corona from a PSPC spectra analysis without *a priori* knowledge of the prevailing coronal abundances, and vice versa. We also show that uncertainties in the intervening interstellar column densities can affect the inferred temperatures and/or abundances. Notwithstanding these difficulties, our analysis confirms that models having similar subsolar abundances to those inferred from *ASCA* and *EUVE* spectra of active coronal stars do indeed produce good fits to PSPC spectra. This general consistency between different instruments implies that explanations for the subsolar abundances that invoke systematic biases due to instrumental effects can now be ruled out. © 1996 American Astronomical Society.

1. INTRODUCTION

X-ray emission from chromospherically active, late-type stars is generally attributed to thermal emission from the hot ($\approx 10^{6.5-7.5}$ K) coronae of these stars. These coronae are significantly hotter, have a much higher emission measure, and, perhaps, are much denser than the solar corona. Such conclusions are based primarily on data collected over the last fifteen years for several thousand coronal-type stars by the *Einstein*, *EXOSAT*, and *ROSAT* x-ray observatories. The primary instruments on these three spacecraft, the imaging proportional counter (IPC), low energy and medium energy (LE+ME) instruments, and the position sensitive proportional counter (PSPC), respectively, obtained low-resolution x-ray spectra of sufficient signal-to-noise (≥ 30) to perform detailed spectral analyses for hundreds of late-type stars. The results of such analyses can be found in Schmitt *et al.* (1990: *Einstein* IPC data), Pallavicini *et al.* (1988: *EXOSAT* LE data), and Dempsey *et al.* (1993: *ROSAT* All-Sky Survey PSPC data for RS CVn binary systems). A major conclusion of these studies is that there is a general trend of increasing coronal temperature T_{cor} with increasing activity, as measured for example by the ratio of the x-ray to the bolometric

luminosity, $R_x = L_x/L_{\text{bol}}$. There also appears to be an inverse correlation between T_{cor} and surface gravity. Jordan *et al.* (1987) and Jordan & Montesinos (1991) have discussed how such correlations can arise for classes of coronal models in which the radiative and conductive energy fluxes are in a fixed ratio. There are some exceptions to these general trends, e.g., the F5 star Procyon has a thin convective zone, an x-ray efficiency R_x similar to that of the Sun, but a coronal temperature of $10^{6.2}$ K, somewhat lower than that of the Sun ($T_{\text{cor}} \approx 10^{6.4}$ K). Other late-A and early-F main-sequence stars also appear to have very soft coronal temperatures (e.g., Simon, *et al.* 1995).

More detailed dependences of coronal properties on environmental parameters, e.g., on binarity (de Medeiros & Mayor 1995), have remained essentially unexplored until recently, due to the small number of high-quality x-ray spectra which have thus far been available. Using data from both our own *ROSAT* Guest Investigator program, as well as from the *ROSAT* Archive, we have assembled x-ray spectra for a small sample of five active stars, which are of moderate to high quality. Included are three active binary systems, one active giant in a very long period binary that can be considered effectively single (i.e., not subject to tidal effects due to its companion star), and an active single giant star. The fundamental properties of these stars are summarized in Table 1.

The three active binary systems studied are IX Per (HD 22124), HR 7428 (V1817 Cyg), and FF Aqr (BD-03°5357).

¹NRC-NASA Senior Research Associate, on leave from Tata Institute of Fundamental Research, Bombay, India.

²Also USRA, Code 610.3, NASA/GSFC.

TABLE 1. Properties of selected chromospherically active stars.

Name	Spectral type ^a	P_{orb}^a (days)	P_{rot}^a (days)	Radius ^a (R_{\odot})	Distance ^a (pc)
HR 7428	A0V+K2 III/III	108.854	~109	62.0	302
HR 9024	G1 IIIe	—	23.25	13.6	175
FF Aqr	G8 III+sdOB	9.208	9.208	6.1	300
29 Dra ^b	K0-2 III+wd	905.9	31.5	7.0	88
IX Per ^c	F5 V + ?	1.326	1.326	1.5	48

^aAll data are from Strassmeier *et al.* (1993) unless otherwise noted.

^bWe have estimated the radius of 29 Dra using the distance and $(V-R)$ color given in Strassmeier *et al.* (1993) and the relation between surface flux and $(V-R)$ derived by Di Benedetto and Rabbia (1987).

^cThe spectral type and orbital period for IX Per are from Eggen (1985). We have estimated the distance to this star assuming an absolute visual magnitude of 3.2. We have estimated the radius of IX Per using this distance, its $(B-V)$ color, and the relation between surface flux and $(B-V)$ given in Barnes *et al.* (1978).

IX Per is an F5 V star in a fairly short-period (1.33 d) binary, which has been classified as an ellipsoidal variable (Morris 1985), but which we consider to be an RS CVn binary system based both on its radio properties (cf. Drake *et al.* 1989) and on its UV spectrum, which displays the same strong high-temperature emission lines as do the RS CVn stars. An analysis of the PSPC data for IX Per has already been presented by Turner *et al.* (1995) who, however, limited themselves to rather simpler x-ray spectral models than the ones we present in this paper. HR 7428 is also both an ellipsoidal variable and a long-period (108.9 d) RS CVn binary. FF Aqr is an interesting 9.2-d period binary, comprised of a G8 III primary and a sdOB secondary star, which was discovered to be eclipsing by Dworetzky *et al.* (1977). The remaining stars, 29 Dra (= DR Dra) and HR 9024 (= OU And), have been classified as active giants on the basis of their rapid rotation rates, UV spectra, and radio emission (see references cited in Strassmeier *et al.* 1993). 29 Dra is the primary of a very wide binary system ($P_{\text{orb}}=904$ days) in which the secondary star is a white dwarf (Fekel & Simon 1985). Fekel *et al.* (1993) have argued that the primary is effectively a single giant, in the sense that its rapid rotation is unrelated to its binarity.

2. OBSERVATIONS

Three of the five active stars listed in Table 1, viz., HR 7428, HR 9024, and FF Aqr, were observed in the course of

the *ROSAT* Guest Observer Program, in pointings that utilized a position sensitive proportional counter (PSPC) as the detector (Truemper 1983; Pfeffermann *et al.* 1987). The PSPC has a field of view of 2° , an energy resolution ($\Delta E/E$) of ≈ 0.42 at 1 keV and a nominal (gain-sensitive) bandwidth of 0.1–2.4 keV. 29 Dra was detected serendipitously as a bright source located $\sim 34'$ away from the center of the field of view in a PSPC observation of an entirely different object. IX Per was also detected as a serendipitous bright source, $\sim 25'$ off-axis, during a PSPC pointing towards the quasar NRAO 140 (Turner *et al.* 1995). At their off-axis positions, neither 29 Dra nor IX Per was obstructed by any mechanical structure in the light path.

We extracted the data from the *ROSAT* archives for the reanalysis presented here. The details of the observations are given in Table 2, which lists the start and end times of the observations, the useful exposure times, the observed count rates and equivalent x-ray fluxes, and the total accumulated counts per spectrum. In each x-ray image, the on-source counts were selected from a circular region on the sky, having a typical radius of about 3.25 (5.7 for 29 Dra and IX Per because of their large offset from field center). The background was accumulated from several neighboring regions at nearly the same offset as the source. These observations resulted in a good quality spectra for 29 Dra and HR 9024, containing over 19000 and 6700 x-ray photons, respectively. The spectra extracted for the other sources were of lower quality, that of IX Per having the smallest number of detected counts (1250), but all were still adequate for the conventional spectral models discussed in the next section.

We have also examined the x-ray source position of FF Aqr and IX Per, both of which are known to have faint companions. In the case of FF Aqr with a 14th mag companion which is $\sim 30''$ away, the x-ray source position is within $8''$ of the optical position of FF Aqr. The 10 mag companion of IX Per on the other hand, is only $\sim 5''$ away and thus within the error circle of the x-ray position. However, according to a high-resolution radio map of the IX Per region (Drake *et al.* 1989), the radio position of IX Per is consistent with its optical position to $\leq 1''$. Therefore, considering the tight correlation between the radio and x-ray emission of RS

TABLE 2. Details of *ROSAT* PSPC observations.

Name		Date				Exposure Time (s)	Mean Count rate & flux ^{a, b}	Total counts ^a
		Y	M	D	UT			
HR 7428	Start	1993	04	11	03:06	24903	0.130 ± 0.002 (1.3)	3250
	End	1993	04	15	17:42			
HR 9024	Start	1993	01	13	08:15	6761	0.993 ± 0.012 (11.6)	6715
	End	1993	01	13	22:46			
FF Aqr	Start	1993	05	08	23:11	5438	0.338 ± 0.008 (3.6)	1840
	End	1993	05	09	15:43			
29 Dra	Start	1992	08	29	11:31	10578	1.81 ± 0.013 (22.3)	19146
	End	1992	08	30	07:30			
IX Per	Start	1992	08	08	17:32	4039	0.309 ± 0.009 ^c (3.0)	1250 ^c
	End	1992	08	08	19:14			

^aCount rates and flux values for PH channels 17–248 corresponding to 0.2–2.4 keV.

^bX-ray flux in brackets is in units of 10^{-12} ergs cm^{-2} s^{-1} .

^cFor PH channels 17–200 corresponding to 0.2–2.0 keV.

TABLE 3(a). Results of spectral analysis using “meka” models.

Parameters	HR 7428	HR 9024	FF Aqr	29 Dra	IX Per
Single-component model with non-solar abundances					
kT(keV)	0.80 ^{+0.04} _{-0.03}	1.11 ^{+0.09} _{-0.07}	0.84 ^{+0.09} _{-0.06}	1.07	0.68 ^{+0.07} _{-0.06}
EM(10^{53} cm ⁻³)	20.2 ^{+3.5} _{-4.0}	75.9 ^{+6.7} _{-6.3}	88.9 ^{+14.5} _{-15.7}	30.1	1.4 ^{+0.4} _{-0.3}
Metallicity (Z)	0.28 ^{+0.09} _{-0.08}	0.17 ^{+0.04} _{-0.04}	0.09 ^{+0.06} _{-0.04}	0.17	0.12 ^{+0.08} _{-0.06}
N_{H} (10^{20} cm ⁻²)	2.6 ^{+0.4} _{-0.4}	4.1 ^{+0.3} _{-0.3}	3.5 ^{+0.4} _{-0.5}	0.8	0.6 ^{+0.4} _{-0.3}
χ^2_{ν} /dof	1.15/25	1.73/25	1.27/25	2.1/23	1.24/18
Two-component model with solar abundances					
kT ₁ (keV)	0.69 ^{+0.04} _{-0.04}	0.64 ^{+0.10} _{-0.25}	0.26 ^{+0.13} _{-0.06}	0.18	0.15 ^{+0.04} _{-0.06}
EM ₁ (10^{53} cm ⁻³)	4.1 ^{+0.8} _{-0.7}	4.6 ^{+3.2} _{-2.8}	3.3 ^{+1.75} _{-0.75}	1.6	0.15 ^{+0.95} _{-0.06}
kT ₂ (keV)	> 1.4	3.0 ^{+3.6} _{-1.2}	1.3 ^{+0.45} _{-0.20}	1.34	0.75 ^{+0.15} _{-0.08}
EM ₂ (10^{53} cm ⁻³)	6.2 ^{+1.5} _{-1.7}	35.9 ^{+3.0} _{-3.2}	24.4 ^{+4.3} _{-3.1}	12.7	0.30 ^{+0.04} _{-0.03}
N_{H} (10^{20} cm ⁻²)	1.4 ^{+0.22} _{-0.16}	2.7 ^{+0.15} _{-0.20}	1.7 ^{+0.64} _{-0.35}	0.35	0.6 ^{+2.8} _{-0.5}
χ^2_{ν} /dof	0.83/24	1.50/24	1.26/24	5.8/22	1.39/17
Two-component model with non-solar abundances					
kT ₁ (keV)	0.74 ^{+0.05} _{-0.04}	0.78 ^{+0.04} _{-0.07}	0.3 ^{+0.35} _{-0.1}	0.86 ^{+0.04} _{-0.06}	0.14 ^{+0.70} _{-0.07}
EM ₁ (10^{53} cm ⁻³)	15.3 ^{+2.2} _{-2.2}	24.4 ^{+8.1} _{-9.7}	6.0 ^{+4.5} _{-2.2}	19.0 ^{+4.7} _{-4.0}	0.30 ^{+6.7} _{-0.20}
kT ₂ (keV)	> 1.8	3.9 ^{+35.5} _{-2.1}	1.1 ^{+0.45} _{-0.2}	> 2.0	0.72 ^{+0.14} _{-0.06}
EM ₂ (10^{53} cm ⁻³)	5.6 ^{+4.4} _{-3.7}	35 ⁺⁵ ₋₇	47 ⁺⁵ ₋₁₀	9.9 ^{+3.0} _{-3.8}	0.78 ^{+0.09} _{-0.09}
Metallicity (Z)	0.30	0.30	0.30	0.18 ^{+0.03} _{-0.03}	0.30
N_{H} (10^{20} cm ⁻²)	2.4 ^{+0.2} _{-0.2}	3.4 ^{+0.2} _{-0.3}	2.5 ^{+0.6} _{-0.3}	0.7 ^{+0.09} _{-0.12}	0.8 ^{+3.0} _{-0.7}
χ^2_{ν} /dof	0.88/24	1.15/24	1.22/24	1.65/21	1.30/17

Note : Errors are with 90% confidence for single parameter ($\chi^2_{\text{min}} + 2.71$), and abundances are relative to solar photospheric values. No errors are given if $\chi^2_{\nu} > 2$.

CVn stars demonstrated by Drake *et al.* (1989), we believe that the x-ray source is indeed physically associated with IX Per.

3. ANALYSIS AND RESULTS

3.1 Spectral Analysis

The *ROSAT* PSPC data were grouped every eight pulse height channels and then fitted. We used the most appropriate PSPC response matrix available: *pspcb_92mar11.rmf* for observations performed before 1991 October 11, and *pspcb_93jan12.rmf* for observations after that date (Turner & George 1994). For the off-axis sources, 29 Dra and IX Per, we created the response matrices based on the available off-axis calibration of the PSPC and using the appropriate ancillary response files. Due to some calibration uncertainties in the response function of the PSPC at very low energies, we ignored the data in the first 16 pulse height channels and chose to fit the data above 0.18 keV only.

We used the XSPEC (Version 9.0) spectral analysis package to fit the data with three different spectral models for thermal-equilibrium plasmas, viz. the Raymond & Smith or RS model (Raymond 1990; Raymond & Smith 1978), the Mewe-Kaastra, or “meka” model (Mewe *et al.* 1985; Kaastra 1992), and the Mewe-Kaastra-Liedahl or “mekal” model (Liedahl *et al.* 1995; Mewe *et al.* 1995). The latter model is an update of “meka” that incorporates recently derived improvements to the Fe L complex atomic data. Except for slight differences in the derived temperatures, the RS and “meka” spectral models gave similar results. The results presented here are thus based on the “meka” and “mekal”

TABLE 3(b). Results of spectral analysis using “mekal” models.

Parameters	HR 7428	HR 9024	FF Aqr	29 Dra	IX Per
Single-component model with non-solar abundances					
kT(keV)	0.96 ^{+0.06} _{-0.05}	1.30 ^{+0.10} _{-0.09}	0.96 ^{+0.11} _{-0.10}	1.25 ^{+0.06} _{-0.06}	0.76 ^{+0.09} _{-0.09}
EM(10^{53} cm ⁻³)	20.9 ^{+3.3} _{-2.8}	72.6 ^{+14.1} _{-5.8}	79.5 ^{+14.1} _{-12.3}	29.4 ^{+1.4} _{-1.3}	1.4 ^{+0.4} _{-0.3}
Metallicity (Z)	0.17 ^{+0.05} _{-0.04}	0.12 ^{+0.05} _{-0.03}	0.06 ^{+0.04} _{-0.03}	0.12 ^{+0.02} _{-0.02}	0.08 ^{+0.05} _{-0.04}
N_{H} (10^{20} cm ⁻²)	2.6 ^{+0.4} _{-0.3}	4.0 ^{+0.3} _{-0.3}	3.3 ^{+0.5} _{-0.4}	0.7 ^{+0.1} _{-0.1}	0.6 ^{+0.4} _{-0.3}
χ^2_{ν} /dof	0.87/25	1.38/25	1.26/25	1.44/23	1.27/18
Two-component model with solar abundances					
kT ₁ (keV)	0.66 ^{+0.16} _{-0.17}	0.39 ^{+0.32} _{-0.10}	0.29 ^{+0.12} _{-0.06}	0.23	0.18 ^{+0.07} _{-0.07}
EM ₁ (10^{53} cm ⁻³)	2.0 ^{+1.1} _{-0.5}	2.7 ^{+0.7} _{-0.6}	5.1 ^{+1.2} _{-1.2}	1.6	0.16 ^{+0.37} _{-0.04}
kT ₂ (keV)	1.8 ^{+3.0} _{-0.4}	2.3 ^{+1.3} _{-0.3}	1.7 ^{+0.5} _{-0.3}	1.8	1.01 ^{+0.18} _{-0.23}
EM ₂ (10^{53} cm ⁻³)	7.6 ^{+1.3} _{-1.1}	36 ⁺¹⁶ ₋₁₆	23.4 ^{+4.7} _{-3.3}	13.4	0.24 ^{+0.05} _{-0.03}
N_{H} (10^{20} cm ⁻²)	1.3 ^{+0.2} _{-0.2}	2.8 ^{+0.3} _{-0.3}	2.0 ^{+0.5} _{-0.4}	0.29	0.6 ^{+1.7} _{-0.3}
χ^2_{ν} /dof	0.93/24	1.43/24	1.23/24	5.2/22	1.49/17
Two-component model with non-solar abundances					
kT ₁ (keV)	0.84 ^{+0.09} _{-0.32}	0.77 ^{+0.16} _{-0.33}	0.31 ^{+0.10} _{-0.10}	See	0.17 ^{+0.15} _{-0.08}
EM ₁ (10^{53} cm ⁻³)	9.1 ^{+5.2} _{-5.3}	8.7 ^{+6.5} _{-4.7}	11.7 ^{+4.0} _{-3.8}	note	0.36 ^{+2.0} _{-0.17}
kT ₂ (keV)	> 1.3	2.1 ^{+1.3} _{-0.5}	1.4 ^{+0.35} _{-0.2}	below	0.91 ^{+0.27} _{-0.13}
EM ₂ (10^{53} cm ⁻³)	7.6 ^{+6.3} _{-3.6}	48 ⁺⁸ ₋₈	39.4 ^{+4.1} _{-4.4}	—	0.60 ^{+0.07} _{-0.10}
Metallicity (Z)	0.30	0.30	0.30	—	0.30
N_{H} (10^{20} cm ⁻²)	2.1 ^{+0.3} _{-0.3}	3.3 ^{+0.2} _{-0.2}	2.6 ^{+0.5} _{-0.4}	—	0.8 ^{+2.3} _{-0.7}
χ^2_{ν} /dof	0.77/24	1.19/24	1.23/24	—	1.34/17

Note : Errors are as in Table 3(a). The best-fit 2T variable abundance model for 29 Dra has zero EM for one of the temperature components and thus is identical to the 1T model.

models for ease of comparison with our previous work on active stars and Algol-type binaries, where we also found somewhat better fits using these models as compared with RS models (Drake *et al.* 1994; Singh *et al.* 1995). We have in general tried single-temperature or isothermal plasma models (hereafter 1T models), and models consisting of two discrete plasma components at different temperatures (2T models). We used these simple spectral models with discrete temperature components rather than more complex models such as continuous emission measure models (CEM), for two reasons: (a) low-resolution, low-bandwidth x-ray spectra with signal-to-noise ratios identical to those of the present spectra cannot distinguish between 2T and CEM models; (b) 2T models provide a convenient characterization of the x-ray spectra in terms of a solar analog (see Singh *et al.* 1996; Antonucci & Dodero 1995). To examine how our conclusions concerning the inferred coronal abundances may have been affected by the adoption of these simple temperature-structure models, we have also tried a 3T solar-abundance model for the source with the best counting statistics, viz. 29 Dra.

The x-ray spectra were fitted with the 1T and 2T plasma models (a) assuming the solar photospheric abundances given in Anders & Grevesse (1989), and (b) allowing the abundance of every element other than H to vary by a common factor Z, hereafter referred to as the metallicity, relative to their solar (photospheric) values. (The energy resolution of the PSPC is insufficient to resolve the contribution of individually varying elements to the plasma emission). In each of the above models, we assumed that the interstellar extinction follows the absorption cross-sections given by

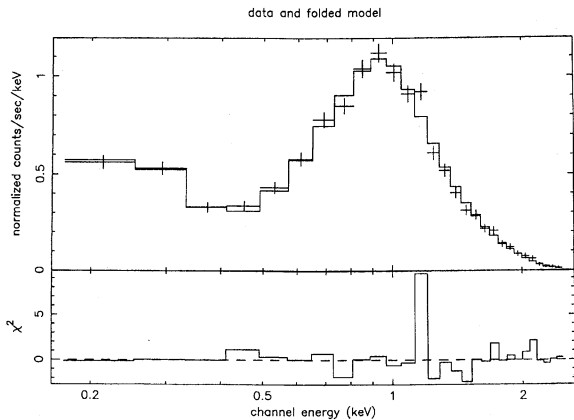


FIG. 1. Upper panel: The observed x-ray spectrum of HR 9024 is shown by the crosses; the best-fit 2T “meka” model folded through the detector response is shown as a histogram. Lower panel: The residuals to the fit are shown in terms of their contribution to the chi-squared statistic.

Morrison & McCammon (1983), and we allowed the total intervening hydrogen column density N_H to vary freely.

We summarize the results of the different model fits in Tables 3(a) (for “meka”) and 3(b) (for “mekal”), listing there the best-fit values and the corresponding 90% uncertainties for each model parameter. Note that for $\nu=24$ degrees of freedom, there is a 90% probability that a fit with a reduced chi-squared value $\chi^2_\nu=1.38$ is unacceptable, and a 95% probability that a fit with $\chi^2_\nu=1.52$ is unacceptable (Bevington 1969). Thus, for the PSPC models described below, we consider those yielding $\chi^2_\nu \geq 1.4-1.5$ as formally unacceptable.

Fits to the PSPC spectra assuming either 1T “meka” or “mekal” models with solar abundances gave unacceptably high values for χ^2_ν and were thus rejected in all cases. However, acceptable 1T fits were achieved using “meka” models for HR 7428, FF Aqr, and IX Per, and using “mekal” models in all five cases, when the abundances were allowed to depart from solar values. The best-fit metallicities for the 1T “meka” models vary from 0.09 for FF Aqr to 0.28 for HR 7428; the best-fit Z values for the “mekal” models are systematically lower than the “meka” values by a factor of one third, ranging from 0.06 to 0.17. The best-fit temperatures derived using the “mekal” models are also systematically higher by 10%–20% than those derived using the “meka” models. Thus, care should be taken when comparing either temperatures or metallicities of coronae inferred using the ‘old’ plasma codes that do not include the Fe L -shell updates with those like “mekal” that do. The values of χ^2_ν for the fits to the HR 9024 and 29 Dra PSPC spectra using the “mekal” code are ~ 1.4 and indicate that the fits, while still formally acceptable, are somewhat poor. However, we have not included any systematic errors in this analysis, notice: addition of a systematic error of a few percent to all the channels would improve the χ^2_ν of these best fits (by about 0.1 in the case of 29 Dra).

We have also obtained fits with about the same values of χ^2_ν for **solar abundance** models using 2T “meka” and “mekal” plasma models for all of the stars except for 29

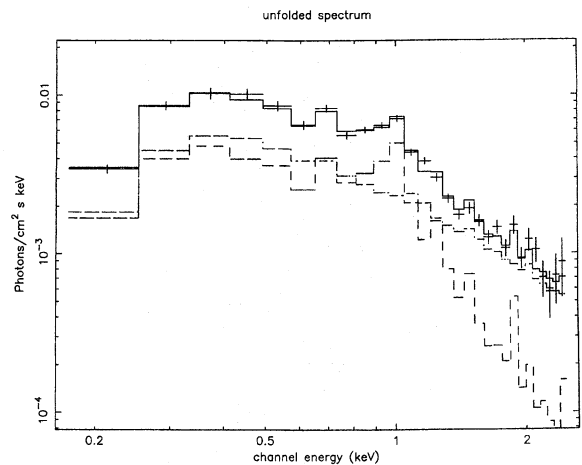


FIG. 2. The unfolded x-ray spectrum of HR 9024 is shown, as well as the best-fit 2T “meka” model with the heavy element abundances set to 0.30 times the solar photospheric value (the solid histogram). The contributions from the 2T components of 0.8 and 4 keV are also shown separately as the dashed histogram.

Dra, for which the fits for both plasma models were highly unacceptable ($\chi^2_\nu=5.8$ and 5.2, respectively). However, an acceptable fit to the 29 Dra spectrum can be obtained with 3T “meka” and “mekal” models constrained to have solar abundances (these model results are not shown in Table 3). Given the few truly independent channels in a PSPC spectrum, complex models of this type having 7 free parameters will almost always find acceptable fits in some region of parameter space; however, the temperatures of the 3 components that we infer using either plasma code are quite plausible, viz. 0.1, 0.7, and 2.6 keV, respectively. We have also made fits using 2T models having subsolar abundances: for 29 Dra (the star with the best signal-to-noise spectrum) we have let the metallicity vary freely, while for the other 4 stars we have fixed it at a value of 0.30 which is typical of the values inferred from analyses of *ASCA* spectra. In all cases, acceptable fits are found (not surprising given that 1T variable abundance models typically have acceptable fits). As noted in Table 3(b), the 2T “mekal” fit for 29 Dra degenerates to the same model as the 1T fit, since one of the components vanishes.

The data for these five stars are thus consistent with either (a) 1T plasma models with highly depleted (0.06–0.30 solar) elemental abundances (with the exception of the “meka” model for 29 Dra for which the $\chi^2_\nu=2.1$), or (b) 2T (3T for 29 Dra) plasma models having solar abundances, or (c) 2T plasma models having subsolar abundances. There is no way on the basis of PSPC spectra alone to choose between these competing classes of models. As an example of one of the fits to the data, we show in Fig. 1 the 2T “meka” fit to the x-ray spectrum of HR 9024. The near-equal contributions of the low-T (0.8 keV) and high-T (4 keV) components are indicated in Fig. 2, where we have plotted the (deconvolved) incident photon spectrum of HR 9024. The allowed ranges of the temperatures with 68%, 90%, and 99% confidence for this particular best-fit model are shown in Fig. 3. The high-T component in the spectrum of HR 9024 is not well-constrained due to the limited high-energy response of

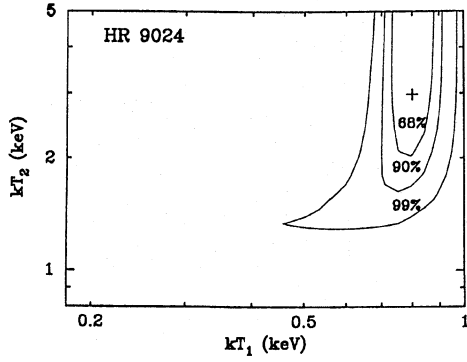


FIG. 3. Allowed ranges of the 2 temperatures in the x-ray spectrum of HR 9024 for 68%, 90%, and 99% confidence based on counting statistics, for the best-fit model shown in Fig. 2.

the PSPC. In Fig. 4, we show similar confidence regions for the two temperature components inferred from our fit to the spectrum of FF Aqr using the “mekal” models. A comparison of the contours in Figs. 3 and 4, shows that there is no overlap of the 90% confidence contours, indicating that the difference in the coronal temperatures for the two stars is significant at a confidence $\geq 90\%$. In fact, in the case of FF Aqr fixing the two temperatures to the values of 0.8 and 3.0 keV as found for HR 9024, gives a much poorer fit with $\Delta\chi^2 = 11.5$. We will discuss the case of FF Aqr in more detail in Sec. 4.

For each of the stars we find that the interstellar absorption column densities N_H deduced from the spectral fits are correlated with the plasma abundances. To examine this influence of N_H on derived abundances, we show the 68%, 90%, and 99% confidence contours for the allowed ranges of N_H and coronal abundances for the “mekal” best-fit models to the spectra of HR 7428, HR 9024, FF Aqr, and IX Per, in Figs. 5(a), 5(b), 5(c), and 5(d) respectively. The results using the “mekal” model (not shown) are very similar to these “mekal” results. The plots are based on 2T models for HR 7428 and HR 9024, and on 1T models for FF Aqr and IX Per. Therefore, the observed effect of inferring low abundances for high values of N_H is independent of whether it is the 1T or the 2T model that is the best fit.

The N_H values for all sources, except HR 7428, are constrained with 99% confidence (see Figs. 5(a)–5(d)). We have compared the values derived by us with the estimates from other measurements. We find that at the 90% confidence level our values compare very well with the estimates compiled by Fruscione *et al.* (1994) and Diplas & Savage (1994), which derive mainly from *IUE* observations of nearby stars. For example, based on the stars closest in space and distance to HR 7428, the value for N_H ranges between $(1-8) \times 10^{20} \text{ cm}^{-2}$, whereas our 90% confidence range is $(1-3) \times 10^{20} \text{ cm}^{-2}$. The similar estimates for HR 9024, FF Aqr, and 29 Dra are $(0.25-8.0) \times 10^{20}$, $(0.45-6.0) \times 10^{20}$, and $(0.3-0.7) \times 10^{20} \text{ cm}^{-2}$, respectively, each of which compares closely with the value resulting from our fit to the *ROSAT* spectrum. No independent estimate of N_H is available for IX Per, but assuming a uniform interstellar density of 0.07 cm^{-3} for the solar neighborhood (Paresce 1984), we get a

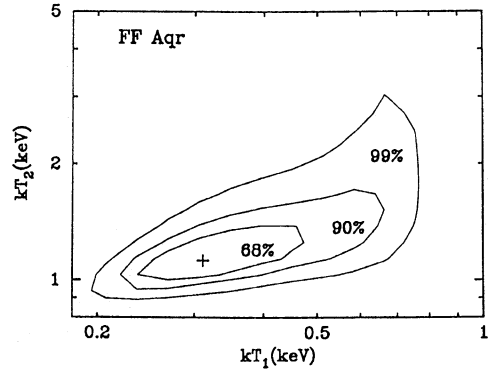


FIG. 4. Allowed ranges of the 2 temperatures in the x-ray spectrum of FF Aqr for 68%, 90%, and 99% confidence based on counting statistics, for the best-fit “mekal” model. The abundance was fixed at 0.3 times the solar photospheric value.

column depth of $\sim 0.2 \times 10^{20} \text{ cm}^{-2}$ for a distance of 87 pc. The 90% confidence lower limit based on our x-ray analysis for this star is $\sim 0.1-4. \times 10^{20} \text{ cm}^{-2}$.

3.2 X-ray Luminosities and Stellar Surface Fluxes

The 0.2–2.4 keV x-ray fluxes for HR 7428, HR 9024, FF Aqr, 29 Dra, and IX Per from the *ROSAT* PSPC observations, and based on the best-fit “mekal” models, are given in Table 2. Their corresponding x-ray luminosities L_x and surface fluxes, $S_x = L_x / (4\pi R_*^2)$, for the active late-type star in all of these systems are given in Table 4. Notice that while IX Per has a factor of 20–50 times lower L_x than the other four stars, this is purely because the active star in this system is a dwarf star, whereas in the other cases the active star is a giant or bright giant. A better measure of coronal strength is the x-ray surface flux, since this quantity does not depend on the stellar surface area. In fact, S_x for IX Per is similar to or greater than that of the other stars in this sample, confirming its status as an active binary system. Conversely, although HR 7428 is a recognized long-period RS CVn binary (albeit one of the longest-period systems for which synchronism appears to have been attained) and has a respectably large L_x , because of its large radius $R_* = 62R_\odot$, its S_x value is about two orders of magnitude smaller than that of the other stars and is, in fact, comparable to that of the active Sun.

4. DISCUSSION

According to our analysis, either 1T models with subsolar abundances or 2T models with a range of abundances, from solar to considerably subsolar, can provide acceptable fits to the x-ray spectra of active late-type stars such as have been analyzed here. In the case of 29 Dra, however, the 2T solar-abundance model cannot acceptably fit the PSPC spectrum, but a 3T (and presumably other more complex temperature models) solar-abundance model can: alternative models which can also fit the 29 Dra spectrum well are (i) a 2T model with subsolar abundances, and (ii) (for the “mekal” model only) a 1T model with subsolar abundances. The subsolar abundances derived using 1T models are typically

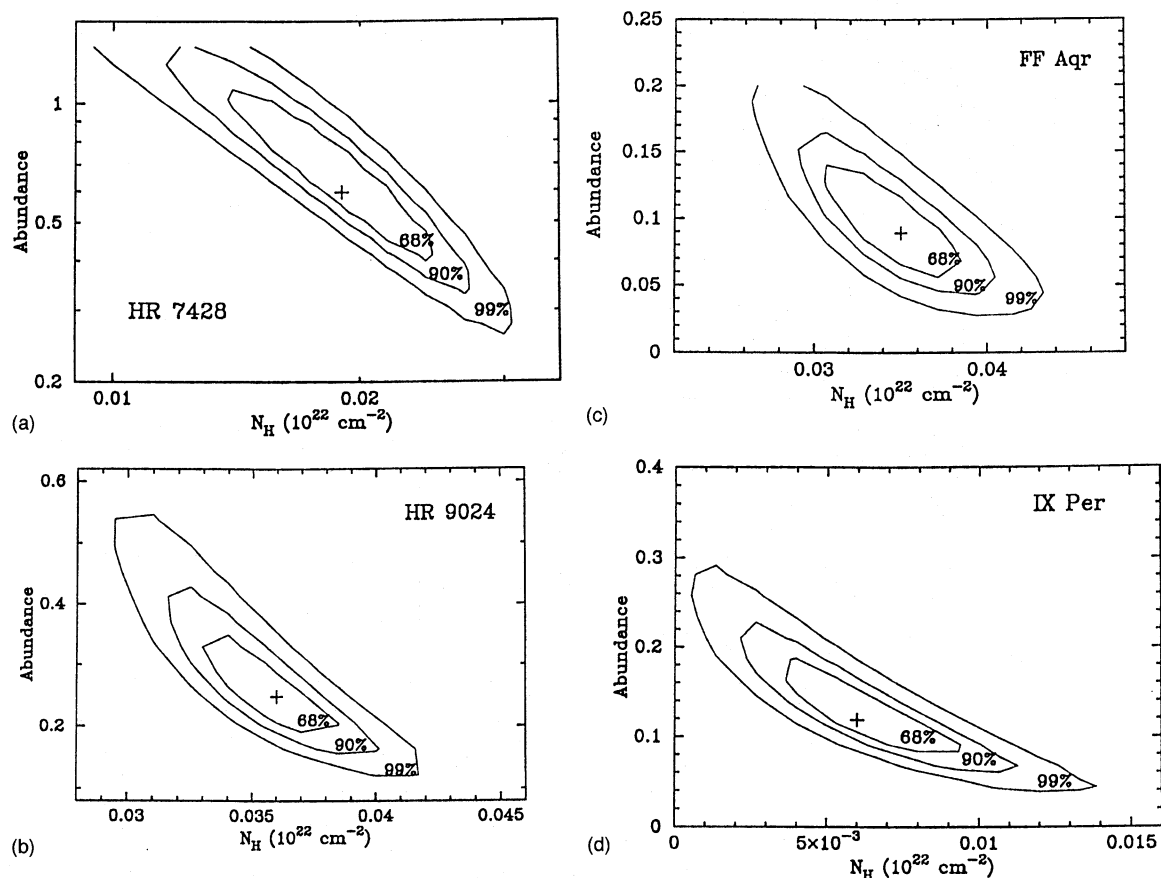


FIG. 5. (a) Allowed ranges for the N_H and elemental abundances from fitting the x-ray spectrum of HR 7428 with 68%, 90%, and 99% confidence based on counting statistics, for the best-fit “mekka” model. (b) Same as (a) for HR 9024. (c) Same as before for FF Aqr, and (d) same as before for IX Per.

0.1–0.3 times the solar photospheric value. Adding a second temperature component with subsolar abundances improves the χ^2_ν of the fit compared to the 1T subsolar models. The low spectral resolution of the PSPC does not allow us to determine which of these contrasting models that give acceptable fits to the observed spectra is the “correct” one. However, we know from the analysis of higher spectral-resolution ASCA spectra of active stars similar to those studied here (e.g., White *et al.* 1994; Antunes *et al.* 1994; Singh 1995; Kaastra *et al.* 1996) that such spectra cannot be fit by solar-abundance plasmas regardless of the form of the coronal temperature distribution, or differential emission measure

(DEM), as it is called. To fit the ASCA spectra of such stars, models with Fe and most of the other heavy elements depleted by a factor of 2–4 compared to their solar photospheric values are typically necessary. Furthermore, such studies have generally shown that the DEM in the temperature range of 10^6 – 10^8 K to which x-ray spectra are sensitive is significantly nonuniform: the best-fit models typically have DEMs that exhibit 2, or possibly 3, peaks and very little emission at other temperatures. Thus, the ASCA modeling suggests that the 2T solar-abundance models that can fit the PSPC spectra of most active stars are not physical in the sense that their goodness of fit is an artifact of the low spectral resolution of the PSPC, and that the models with subsolar abundances are in fact the correct ones.

The spectral parameters for the corona of 29 Dra derived by Dempsey *et al.* (1993), based on 2T solar-abundance models, agree with those derived here and shown in Table 3 for the same model. The much better signal-to-noise of the data used here from a *ROSAT* pointing observation, as compared to the *ROSAT* Sky Survey data used by Dempsey *et al.* (1993), however, effectively rules out a 2T solar-abundance model in this case. An effect of using nonsolar abundance models is to raise the coronal temperatures derived compared to the values derived assuming solar abundances, as can be

TABLE 4. X-ray and UV properties of selected chromospherically active stars.

Name	L_x^a $10^{30} \text{ erg s}^{-1}$	S_x^a $10^7 \text{ erg cm}^{-2} \text{ s}^{-1}$	X-ray deficit ^b dex
HR 7428	14.0	0.007	–0.45
HR 9024	43.0	0.38	–0.17
FF Aqr	34.2	1.50	–0.78
29 Dra	20.6	0.70	0.30
IX Per	0.83	0.61	–0.73

^aPresent measurements in the 0.2–2.4 keV energy band.

^bFrom C IV and x-ray fluxes corrected for reddening.

seen in Table 3, and in other previously analyzed higher resolution spectra of HR 1099 (Drake *et al.* 1996) and AR Lac (Singh *et al.* 1996), as well as in our ongoing analyses of a number of RS CVns in the *ROSAT* public database.

The coronal temperatures of HR 9024, a single giant star, are similar to those found in classical RS CVn binaries like AR Lac (White *et al.* 1994; Swank *et al.* 1981) and HR 1099 (Drake *et al.* 1996), or Algol-type binaries (Antunes 1994; Singh *et al.* 1995). This suggests that, at least to the limited temperature resolution of the PSPC, the coronal DEMs of active stars are identical, regardless of whether they are single or binary stars. The PSPC spectra of FF Aqr, and also (with less significance) that of IX Per, are somewhat softer than the other spectra, inasmuch as they show evidence for a component with a temperature of $\sim 0.2\text{--}0.3$ keV, whereas the lowest temperature inferred for the other stars is $\sim 0.8\text{--}1.0$ keV. A similarly soft coronal DEM has been derived from the analysis of *ASCA* spectra of the much less x-ray luminous single stars β Cet and π^1 UMA, and of the nonsynchronous binary system Capella (Drake *et al.* 1994). Since FF Aqr is the strongest x-ray emitter in our sample as measured by its x-ray surface flux S_x (see Table 4), its relative softness appears to contradict the x-ray activity/coronal temperature trend for coronal-type stars that was mentioned in Sec. 1. It should be borne in mind, however, that the coronal temperatures of FF Aqr (and IX Per) have been derived here from PSPC spectra with relatively small number of counts and very low-resolution, and need to be confirmed, preferably from higher signal-to-noise and spectral-resolution data.

Despite the fact that HR 7428 has a very low S_x , one that is ~ 100 times less than the values for the other stars in our sample (see Table 4), its coronal temperatures are quite similar to those of the other, more chromospherically active stars. This suggests that the relationship between x-ray surface flux and coronal temperature structure may not be as simple as previously inferred. For example, the active Sun has a typical x-ray luminosity of $10^{27.5}$ erg s $^{-1}$, equivalent to an average x-ray surface flux of $\sim 5 \times 10^4$ erg cm $^{-2}$ s $^{-1}$, which is nearly identical to the value we infer for HR 7428. However, the typical temperature of the active solar corona is only $\sim 0.4\text{--}0.6$ keV, while that of HR 7428 is $\sim 0.7\text{--}3.0$ keV, according to our present results. It is possible, therefore, that the latter is indicating that giant stars with low surface gravities, g , have higher-temperature coronae than do otherwise similar dwarf stars with higher gravities. This gravity-dependence of the coronal temperature T_{cor} was first suggested by Schmitt *et al.* (1990), based on their analysis of *Einstein* IPC spectra of a large number of late-type stars, including both single stars and active binaries. Jordan & Montesinos (1991, hereafter JM91), have shown how such a temperature trend naturally arises if the energy density of the corona is directly proportional to the magnetic energy density, and they have inferred a scaling law of the form $T_{\text{cor}} \propto g^{-0.5} \text{Ro}^{-1}$, where Ro is the Rossby number (the ratio of the rotational period P_{rot} to the convective turnover time τ_C : Noyes *et al.* 1984). This gravity dependence could be the reason why the corona of the dwarf star IX Per may be cooler than that of HR 9024, despite the fact that they have

similar Rossby numbers (~ 0.7). The observed ratio of the high-temperature components for these two stars is only 4.3, however, consistent with a shallower dependence ($g^{-0.24}$) than that predicted by the JM91 relation. The low coronal temperature of FF Aqr, however, neither agrees with the general results found by Schmitt *et al.* (1990) nor with the prediction using the JM91 relation that it have a T_{cor} as high as those of the other giant stars, since the active star in FF Aqr is also a giant. This binary is discussed in more detail below.

Another way of examining whether the coronal temperature structures of any of these stars is unusual has been discussed by Simon & Drake (1989) (cf. also Ayres *et al.* 1995), and involves a comparison of the observed (reddening-corrected) C IV $\lambda 1550$ resonance line flux as measured by *IUE* with the x-ray flux. These authors showed that, while most active stars exhibit a fairly tight power-law correlation (the ‘‘Rossby relation’’) between these two quantities, there are some stars that appear to be x-ray deficient, in that their observed x-ray fluxes are much smaller than predicted from their observed C IV fluxes using the Rossby relation. For example, many F0–F5 dwarf and subgiant stars have x-ray deficits of 0.5 to 2.0 dex. We have used the Rossby relation of Simon *et al.* (1985), published and unpublished C IV flux measurements made by *IUE*, and the observed x-ray fluxes given in Table 2, to calculate the x-ray deficits for the five stars in the present sample; these are listed in Table 4. The scatter in the Rossby relation is such that only x-ray deficits of ≥ 0.5 dex are significantly in disagreement with the mean relation (thus, HR 7428, HR 9024, and 29 Dra have small x-ray deficits that imply their x-ray fluxes are fairly consistent with the Rossby relation). As might have been expected, the F5 V star IX Per shows a noticeable x-ray deficit of -0.73 dex, similar to that found by Simon & Drake (1989) for other F stars, e.g., the F5 IV–V star Procyon which has an x-ray deficit of -0.93 dex. (The physical significance of this effect in the early F stars is discussed in some detail in Simon & Drake). However, the star in our sample with the largest x-ray deficit of -0.78 dex is the same system which appeared somewhat anomalous in its coronal temperature structure, the active giant binary system FF Aqr. These two pieces of evidence taken together suggest that the differential emission measure distribution of transition region and coronal material in this binary is systematically skewed to lower temperatures compared to other active dwarf and giant stars.

Why might FF Aqr be anomalous in x-rays? FF Aqr is an eclipsing binary system containing a G8 III (or III–IV) star and an OB subdwarf with an effective temperature of $\sim 3.5\text{--}4.0 \times 10^4$ K with a relatively short 9.21-d orbital period. Since the less evolved G star is four times more massive than the subdwarf star (Dworetzky *et al.* 1977), this system has clearly had significant mass transfer between the two component stars, and is in a rather different evolutionary state than typical (detached) RS CVn stars of this orbital period. The G giant in this system appears to be rotating synchronously with its orbital motion, and, consequently, has high levels of activity, as shown by its strong H α and Ca II H-K emission (Dworetzky *et al.* 1977), UV emission lines of C II, C IV, N V, and Mg II (Dorren *et al.* 1982; Baliunas *et al.*

1986), and radio continuum emission (Drake *et al.* 1989). The broad-band optical continuum of FF Aqr (outside of eclipse) also shows a near-sinusoidal variation with an amplitude of about 0.3 mags, the nature of which is still unclear. Dworetzky *et al.* (1977) attributed it to a reflection effect, but most authors since then (e.g., Dorren *et al.* 1983) have interpreted it as a photometric wave effect due to a nonuniform coverage of the G giant's surface by starspots like those in most RS CVn-type binaries. Recently, the suggestion that some or all of the G star's activity is due to the irradiation of its atmosphere by the hot subdwarf secondary has been revived (Marilli *et al.* 1995). Furthermore, Baliunas *et al.* (1986) have presented evidence that there is a significant geometrical extension (of up to 1.5 G star radii) of absorbing material around the G giant in this binary system, as inferred from strong orbital phase-dependent absorption seen in its C II and C IV lines: these authors suggest that this might be due to absorption features formed in tall loops rather than due to a wind from the G giant. There is also no evidence for an ellipticity effect in the optical photometry and therefore, it is unlikely that the G star is filling its Roche lobe and contributing to a direct mass transfer.

It was partly because of the above-summarized properties that FF Aqr was initially selected as part of our *ROSAT* PSPC observing program, despite the absence of any previous x-ray measurement. It is tempting to attribute the atypical coronal temperature structure of this binary star as being the consequence of some (or all!) of its confirmed or suspected peculiar properties. For example, in addition to coronal plasma heated by the standard dynamo effect, there may be material heated to transition region and/or coronal temperatures in either shocked regions related to mass transfer between the primary and compact secondary, or in the outer atmosphere of the primary that is being irradiated by the hot secondary component, since the thermal structure of a photoionized plasma is expected to be very different from that of a collisionally ionized plasma. Before detailed modeling is warranted, however, we feel higher quality spectra of this interesting system are necessary: since its intervening column density is so large as to preclude observation in the EUV range, soft x-ray spectra of higher energy resolution and wider energy range as can be obtained with *ASCA* would be useful and have been scheduled.

5. CONCLUSIONS

Our analysis of the PSPC x-ray spectra of five chromospherically active stars, HR 7428, FF Aqr, IX Per, 29 Dra, and HR 9024, has shown that spectral models with

1-temperature or 2-temperature plasma components and subsolar (by factors of $\sim 3-10$) abundances can provide good fits to the observed spectra. Such models have previously been found to give good fits to *ASCA* spectra of similar active stars, and to simultaneously obtained *ASCA* and PSPC spectra of the RS CVn binary AR Lac (Singh *et al.* 1996). It is encouraging that analyses of PSPC and *ASCA* spectra of active stars have yielded compatible best-fit models, since this suggests that the inferred subsolar abundances cannot now be plausibly attributed to some kind of systematic instrumental problem, for example, with the *ASCA* spectrometers. The PSPC spectra can also be fit by 2T (3T for 29 Dra) models constrained to have solar abundances. This illustrates the difficulty in independently deriving the temperature structure and the abundances from PSPC spectra alone. The spectrum of FF Aqr, a late-type giant with a sdOB companion, seems somewhat softer than that of the other active giant stars in the sample. A similar softness is also indicated in the spectrum of the F dwarf binary star IX Per but is of lower statistical significance. In contrast, the stars 29 Dra, HR 7428, and HR 9024 have high-temperature coronae, which appear very similar to those of other active binaries, such as AR Lac and Algol. We have considered possible explanations for the soft coronal temperatures in FF Aqr, and speculated that it may be related to the unusual binary configuration of this system, but additional higher quality x-ray spectra are required to solve this puzzle.

Note added in proof: A recent paper by Bauer & Bregman (1996, *ApJ*, 457, 382) also discusses the fitting of PSPC spectra using plasma emission models, and the correlation between metallicity, temperature, and absorption column. Both their study and the present paper, although they differ in some respects, demonstrate that it is difficult to derive reliable elemental abundances based on PSPC spectra alone.

We thank the entire *ROSAT* team for making these observations possible. We also thank Jelle Kaastra, Rolf Mewe, and Duane Liedahl for their work in producing the updated plasma code which is incorporated into XSPEC as the "mekal" model. We thank the referee, Dr. Jeffrey Linsky, for his constructive criticism of an earlier version of this paper. This research has made use of *ROSAT* archival data obtained through the High Energy Astrophysics Science Archive Research Center, HEASARC, Online Service, provided by the NASA-Goddard Space Flight Center, as well as the Simbad database, operated by CDS in Strasbourg, France.

REFERENCES

- Anders, E. & Grevesse, N. 1989, *Geochim. Cosmochim. Acta*, 53, 197
 Antonucci, A., & Doderio, M.A. 1995, *ApJ*, 438, 480
 Antunes, A., Nagase, F. & White, N.E. 1994, *ApJ*, 436, L83
 Ayres, T.R., *et al.* 1995, *ApJS*, 96, 223
 Baliunas, S.L., Loeser, J.G., Raymond, J.C., Guinan, E.F., & Dorren, J.D. 1986, *New Insights in Astrophysics*, ESA SP-263, p. 185
 Barnes, T.G., Evans, D.S., & Moffett, T.J. 1978, *MNRAS*, 183, 285
 Bevington, P.R. 1969, *Data Reduction and Error Analysis for the Physical Sciences* (McGraw-Hill, New York)
 de Medeiros, J.R., & Mayor, M. 1995, *A&A*, 302, 745
 Dempsey, R.C., Linsky, J.L., Schmitt, J.H.M.M., & Fleming, T.A. 1993, *ApJ*, 413, 333
 Di Benedetto, G.P., & Rabbia, Y. 1987, *A&A*, 188, 114
 Diplas, A., & Savage, B.D. 1994, *ApJS*, 93, 211
 Dorren, J.D., Guinan, E.F., & Siah, M.J. 1983, *IBVS* No. 2305

- Dorren, J.D., Guinan, E.F., & Sion, E.M. 1982, *Advances in Ultraviolet Astronomy: Four Years Of IUE Research*, NASA CP-2238, p. 517
- Drake, S.A., Simon, T., & Linsky, J.L. 1989, *ApJS*, 71, 905
- Drake, S.A., Singh, K.P., & White, N.E. 1996, in *Astrophysics in the Extreme Ultraviolet*, Proceedings of IAU Colloquium 152, edited by S. Bowyer and R.F. Malina (Kluwer, Dordrecht), p. 147
- Drake, S.A., Singh, K.P., White, N.E., & Simon, T. 1994, *ApJ*, 436, L87
- Dworetzky, M.M., Lanning, H.H., Etzel, P.B., & Patenaude, D.J. 1977, *MNRAS*, 181, 13P
- Eggen, O.J. 1985, *PASP*, 97, 807
- Fekel, F.C., Henry, G.W., Busby, M.R., & Eitter, J.J. 1993, 106, 2370
- Fekel, F.C., & Simon, T. 1985, *AJ*, 90, 812
- Fruscione, A., Hawkins, I., Jelinsky, P., & Wiercigroch, A. 1994, *ApJS*, 94, 127
- Jordan, C., Ayres, T.R., Brown, A., Linsky, J.L., & Simon, T. 1987, *MNRAS*, 225, 903
- Jordan, C., & Montesinos, B. 1991, *MNRAS*, 252, 21P
- Kaastra, J.S., 1992, *An X-ray Spectral Code for Optically Thin Plasmas* (SRON-Leiden Report, updated version 2.0)
- Kaastra, J., Mewe, R., Liedahl, D.A., Singh, K.P., White, N.E., & Drake, S.A. 1996, *A&A*, submitted
- Liedahl, D.A., Osterheld, A.L., & Goldstein, W.H. 1995, *ApJ*, 438, L115
- Marilli, E., Frasca, A., Bellina Terra, M., & Catalano, S. 1995, *A&A*, 295, 393
- Mewe, R., Gronenschild, E.H.B.M., & van den Oord, G.H.J. 1985, *A&A*, 62, 197
- Mewe, R., Kaastra, J.S., & Liedahl, D.A. 1995, *Legacy*, 6, 16
- Morris, S.L. 1985, *ApJ*, 295, 143
- Morrison, R., & McCammon, D. 1983, *ApJ*, 270, 119
- Noyes, R. W., Hartmann, L. W., Baliunas, S. L., Duncan, D. K., & Vaughan, A. M. 1984, *ApJ*, 279, 763
- Pallavicini, R., Monsignori-Fossi, B. C., Landini, M., & Schmitt, J. H. M. 1988, *A&A*, 191, 109
- Paresce, F. 1984, *AJ*, 89, 1022
- Pfeffermann, E., *et al.* 1987, *Proc. SPIE Int. Soc. Opt. Eng.*, 733, 519
- Raymond, J.C. 1990 (private communication)
- Raymond, J.C., & Smith, B.W. 1978, *ApJS*, 35, 419
- Schmitt, J.H.M.M., Collura, A., Sciortino, S., Vaiana, G.S., Harnden, Jr. F.R., & Rosner, R. 1990, *ApJ*, 365, 704
- Simon, T., Boesgaard, A. M., & Herbig, G. 1985, *ApJ*, 293, 551
- Simon, T., & Drake, S.A. 1989, *ApJ*, 346, 303
- Simon, T., Drake, S.A., & Kim, P.D. 1995, *AJ*, 107, 1034
- Singh, K.P., Drake, S.A., & White, N.E. 1995, *ApJ*, 445, 840
- Singh, K.P., White, N.E., & Drake, S.A. 1996, *ApJ* (in press)
- Strassmeier, K.G., Hall, D.S., Fekel, F.C., & Scheck, M. 1993, *A&AS*, 100, 173 (CABS2)
- Swank, J.H., White, N.E., Holt, S.S., & Becker, R.H. 1981, *ApJ*, 246, 208
- Truemper, J. 1983, *Adv. Space Res.*, 2, 241
- Turner, T.J., & George, I.M. 1994, *ROSAT PSPC Calibration Guide*, Documentation available at US *ROSAT* Science Data Center & HEASARC
- Turner, T.J., George, I.M., Madejski, G.M., Kitamoto, S., & Suzuki, T. 1995, *ApJ*, 445,
- White, N.E., *et al.* 1994, *PASJ*, 46, L97